Article

Optimization of Small Horizontal Axis Wind Turbines Based on Aerodynamic, Steady-State, and Dynamic Analyses

Khalil Deghoum [1,2], Mohammed Taher Gherbi [2], Hakim S. Sultan [3], Adnan N. Jameel Al-Tamimi [4], Azher M. Abed [5], Oday Ibraheem Abdullah [6,7,8,*], Hamza Mechakra [9] and Ali Boukhari [2]

[1] UDERZA Laboratory, University of El Oued, El Oued 39000, Algeria
[2] Department of Mechanical Engineering, University of El Oued, El Oued 39000, Algeria
[3] College of Engineering, University of Warith Al-Anbiyaa, Karbala 56001, Iraq
[4] College of Technical Engineering, Al-Farahidi University, Baghdad 10001, Iraq
[5] Air Conditioning and Refrigeration Techniques Engineering Department, Al-Mustaqbal University College, Babylon 51001, Iraq
[6] Energy Engineering Department, College of Engineering, University of Baghdad, Baghdad 10071, Iraq
[7] Mechanical Engineering Department, College of Engineering, Gulf University, Sanad 26489, Bahrain
[8] Institute of Laser and Systems Technologies (iLAS), Hamburg University of Technology (TUHH), Harburger Schloßstraße 28, 21079 Hamburg, Germany
[9] Dynamics of Engines and Vibroacoustic Laboratory, F.S.I., M'Hamed Bougara University of Boumerdes, Boumerdes 35000, Algeria
* Correspondence: oday.abdullah@tuhh.de

Abstract: In this article, the model of a 5 kW small wind turbine blade is developed and improved. Emphasis has been placed on improving the blade's efficiency and aerodynamics and selecting the most optimal material for the wind blade. The QBlade software was used to enhance the chord and twist. Also, a new finite element model was developed using the ANSYS software to analyze the structure and modal problems of the wind blade. The results presented the wind blade's von Mises stresses and deformations using three different materials (Carbon/epoxy, E-Glass/epoxy, and braided composite). The modal analysis results presented the natural frequencies and mode shapes for each material. It was found, based on the results, that the maximum deflections of E-glass, braided composite and carbon fiber were 46.46 mm, 33.54 mm, and 18.29 mm, respectively.

1. Introduction

The world is moving rapidly towards using renewable energies to reduce dependency on fossil fuels to reduce emissions and pollution. One of the important renewable energy sources is wind energy, which is available for free and sufficient in many places around the world. Wind turbines are widely used worldwide to produce electricity from wind energy. This energy can be used in different applications and fields, such as agriculture and factories, as well as supplying homes with electricity [1]. According to the World Wind Energy Association (AWEA) report, the demand for wind energy is growing quickly worldwide. The installed capacity of wind turbines in all countries of the world for the year 2021 is approximately 840 GW, with increasing of 97.3 GW compared to the year 2020 [2]. The blade is one of the most important components of the wind turbine, as it is responsible for rotating the generator shaft to produce the power. Wind and gravitational loads are some of the biggest problems a blade faces during its lifetime. For this reason, many researchers investigate how to improve the blade's design and manufacturing material so that it is more resistant to external factors. Wind turbine blade design is essential for obtaining high efficiency, where improving the blade's aerodynamic characteristics is considered the main key.

Rašuo and Bengin [3] used the Genetic Algorithm method to optimize the power production of a single wind turbine by shifting its location in a wind farm to avoid the influence of vortex and free wakes between them. Norouzi and Bozorgian [4] worked on a new system for wind turbines called Wind Thermal Energy Systems (WTES). This system relies on generating thermal energy through simple and light electric brakes at the top of the tower. It depends on the wind in the rotation process, and the energy coefficient reached 62.5%. Yee Win and Thianwiboon [5] used experimental and numerical methods to study the ground effect on the Naca 4412 airfoil in order to optimize the parameters for different angles of attack. Mousavi et al. [6] used OpenFOAM to simulate the Subsonic turbulent flow over the NACA0012 airfoil at various Reynolds numbers. They focused mainly on the transitional and turbulent regions and extracted the velocity and pressure distributions for different angles of attack. Garcia-Ribeiro et al. [7] used the experimental and CFD simulation to investigate the effect of the taper ratio of winglets on the performance of a Horizontal Axis Wind Turbine (HAWT). Bai and Wang [8] investigated the aerodynamic performance of a small HAWT using experimental and numerical methods (CFD and BEM). Maizi et al. [9] applied computational fluid mechanics (CFD) to optimize the shape of Horizontal Axis Wind Turbine (HAWT) NREL with different blade tip ratios. Kaya et al. [10] designed a 0.9 m HAWT blade and optimized the aerodynamic performance using a numerical simulation CFD. Parezanovic et al. [11] applied the CFD, and Xfoil software to optimize the wind turbine blade airfoil by choosing three different types. In their study, the lift and drag coefficients were calculated and compared with the experimental results.

Creating a new wind turbine structure is complicated because of the difficulty of designing and choosing the optimal material. In modern wind turbines, composite materials are selected for their lightweight and high strength/stiffness to withstand the impact. In addition to their increased safety and reliability, as well as being recyclable and environmentally friendly [12]. Due to its extreme importance, many studies are concerned with designing and developing the wind turbine blade structure. Lipian et al. [13] used the experimental and fluid-structure interaction simulation to study a small wind turbine's deformations and stresses of 350 W. Boudounit et al. [14] simulated the offshore wind turbine blade using the finite element method (ABAQUS software) under different wind speeds. A comparison was made between the glass and carbon fiber materials to reduce the turbine weight. Also, they optimized the structure by studying the displacements, and von mises stress to determine the damaged area of the blade using each material. Abdullah et al. [15] studied the dynamic problem of the composite material of the rotating blade and the structure by applying the finite element method. Altmimi et al. [16] optimized the blade of the small wind turbines and studied the aero-structural design. Tüfekci et al. [17] investigated the core and multiple layers of composite materials of DTU-10MW-RWT wind turbine blades. The modal and structural problems were studied by applying the Finite Element Method. The composite blades' mode shapes and natural frequencies were found (edgewise bending, flapwise bending, torsional bending, and coupled the flapwise edgewise). Navadeh et al. [18] used the Finite Element Method (both ABAQUS and ANSYS packages) to analyze the vibrations of the wind turbine blade based on longleaf pine and UD composite skin material. Lagdani et al. [19] compared the results of Vibration for carbon and glass epoxy materials of the wind turbine to obtain the characteristics of the dynamic response under the effect of different ice thicknesses.

This study aims to design a new mathematical model of the small wind turbines of 5 kW, and optimize the aerodynamic characteristics of the new proposed model. This part focused on enhancing the power coefficient and power of wind turbines. The second part of the work investigated the selection process of the optimal material for wind blades to improve the strength and stiffness of the structure. The deformations of the tip and natural frequencies were considered as the criterion to optimize the wind blade. Figure 1 shows the main step developed in this work to optimize the wind turbine blade.
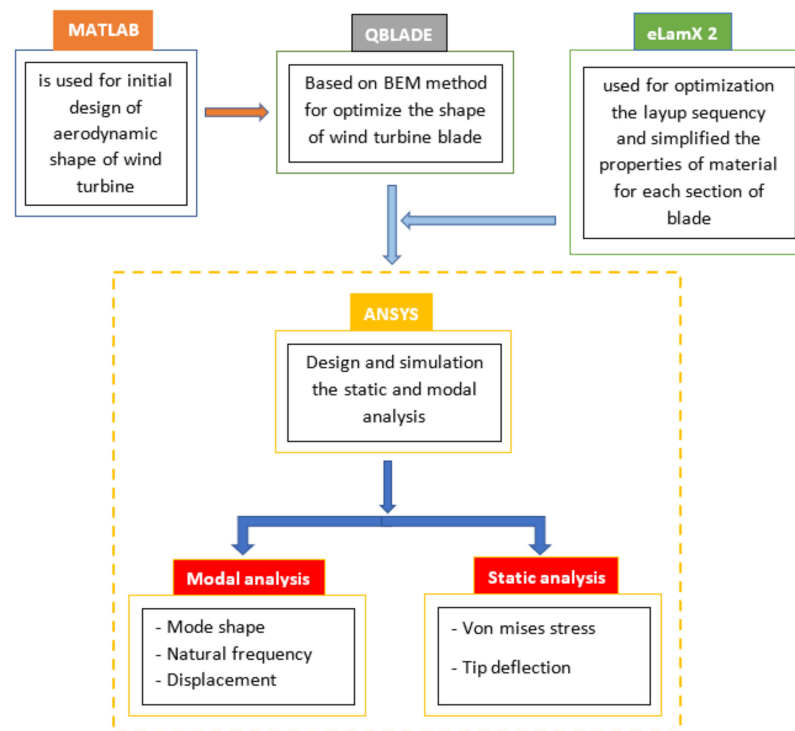
Figure 1. The main steps to optimize small wind turbines.

2. Structural Analysis and Design of the Blade

2.1. Wind Turbine Blade Design

Designing the shape of the wind turbine blade is one of the most complex and important steps in order to manufacture a wind turbine blade. Firstly, the pitch-regulated turbines were selected based on the design of a single airfoil (NACA 4412). This airfoil is well-established, tested, and used for small wind turbine blades [20]. There are many theories to predict aerodynamic performance to calculate the ideal chord length and the optimal twist angle distribution [21]. The simplest model of the ideal concept for wind turbine blade design was developed by Betz [22]. In order to obtain the optimum aerodynamic design of the blade, it was applied the blade element momentum theory (BEM) [8]. Where QBlade software is built based on the BEM theory [23]. This software is used to optimize the shape of the wind blade and determine the aerodynamic loads.

A new code was developed using MATLAB software based on the Betz concept to calculate the parameter of the blade geometry (relative angle (φ), chord length (c), twist angle (θ)). Then, all the parameters are transferred to QBlade software to estimate the load and performance of the blade based on the BEM method. Figure 2 shows the aerodynamic loads for each blade element. BEM theory splits the blade into a finite number of independent sections that are uniformly distributed along the blade's length. A two-dimensional airfoil was used to determine the aerodynamic forces that were generated in each blade section based on a certain radial position. In this work, the blade is divided into 10 sections. The first step in QBlade is to calculate the airfoil's coefficients (lift and drag), where the lift and drag are affected by the Reynolds number (*Re*) and the angle of attack. Reynolds number is defined as the ratio between the inertial force to the viscous force, which is given by the following equation [21]:

$$Re = \frac{\rho U_{rel} c}{\mu} \tag{1}$$

and

$$U_{rel} = \sqrt{(\Omega R)^2 + \left(U_{design}\right)^2} \tag{2}$$

where μ is the air viscosity, U_{rel} is the relative velocity [m/s], c is the chord length [m], Ω is the rotational speed of the blade [rad/s], R is the blade length [m], and U_{design} is the design wind speed [m/s]. The design parameters of the actual blade are listed in Table 1.
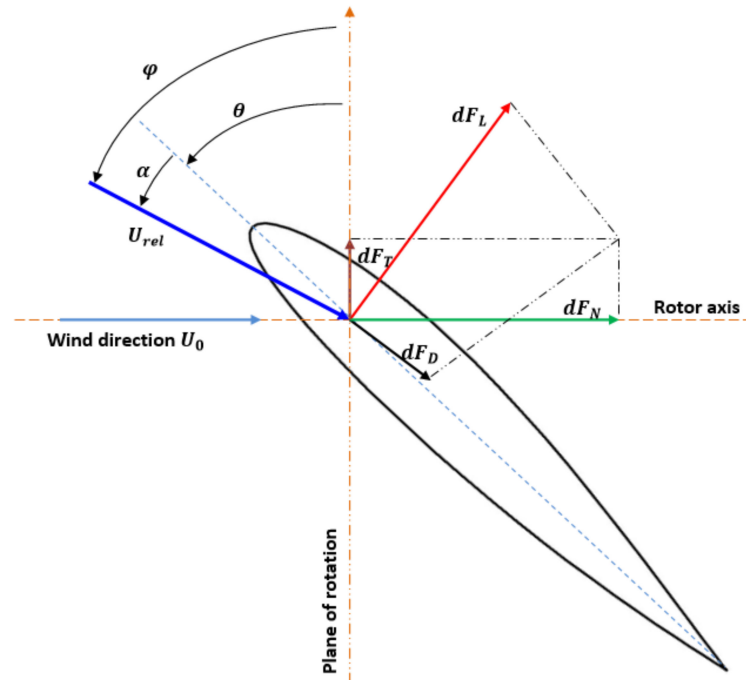

Figure 2. Airfoil section with aerodynamic loads.

Table 1. Initial design parameters of 5 kW small wind turbine.

| Design Parameter	Value	Unit
Rated power	5	[kW]
Design Wind speed	10.5	m/s
Number of blades	3	[-]
Design tip speed ratio	6	[-]
Design angle of attack	6	[°]
Rotor radius	2.5	[m]
Design rotational speed	240	[rpm]
Density of air	1.22	[kg/m^3]
Airfoil type	NACA4412	[-]

According to Equation (1), the Reynolds number changes in terms of the chord (c) and the radius (r). Therefore, it is difficult to determine the initial value to start the calculation process, so it assumed the average value of the Reynolds number to facilitate the calculation process of a 5 kW HAWT with a rotor diameter of 5 m. It was found that the value of Reynolds number is about 450,000 at the tip chord of 0.106 m of the blade. In order to calculate the lift and drag coefficients, the XFoil software was used. Where the XFoil is embedded in QBlade, and the results are shown in Figure 3. The maximum ratio Cl/Cd is 119 at the angle of attack (AOA) which is equal to 6°. This angle is called the design or optimal angle of attack. The lift coefficient at the optimal angle is $Cl_{,design} = 1.12$. can be used to find the relative angle [21]:

$$\varphi = \left(\frac{2}{3}\right) \tan^{-1}\left(\frac{1}{\lambda_r}\right) \tag{3}$$

and

$$\lambda_r = \lambda_0(r/R) \tag{4}$$
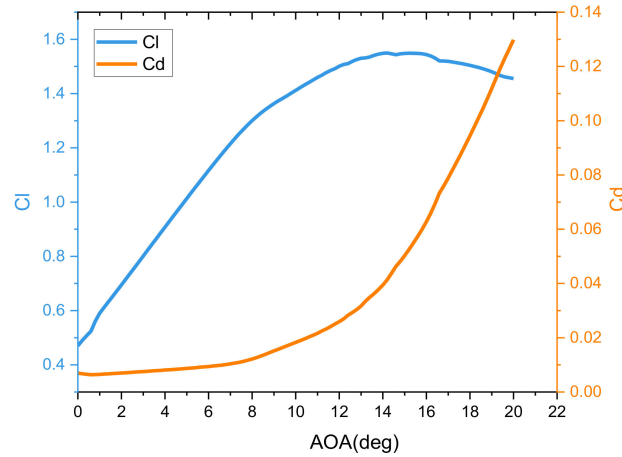
Figure 3. The variation of Lift (*Cl*) and drag (*Cd*) coefficients with the angle of attack.

The chord length in each section can be found as follows,

$$c = \frac{8\pi r}{BC_{l,design}}(1 - \cos\varphi) \tag{5}$$

and the twist angle is,

$$\theta = \varphi - \alpha_{opt} \tag{6}$$

where λ_r is the local speed ratio of the blade, r is the distance from the blade section to the rotor center [m], α_{opt} is the optimal angle of attack, and λ_0 is the design tip speed ratio, which is equal to 6. The 3D distribution of the blade element section, chord length, and twist angle are shown in Figure 4.
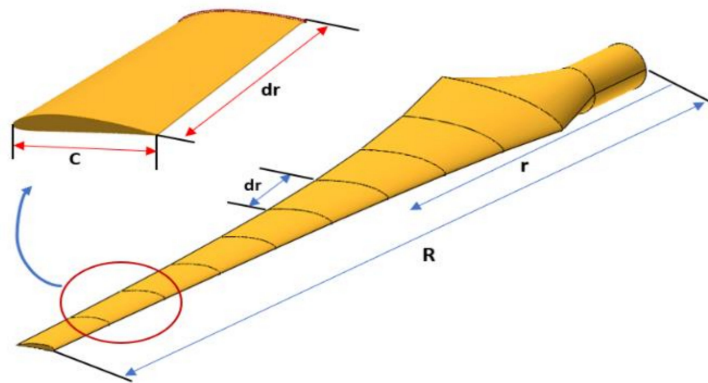
Figure 4. Schematic of blade sections.

2.2. Blade's Material and Lay-Up Sequence

The blades of a small wind turbine are manufactured from several materials; among the most common typical materials are E-glass/epoxy, S-glass/epoxy, carbon/epoxy, braided composite, aluminum, etc. Because of the diversity of materials used to manufacture the wind turbine blade, it was selected in this study the most typical materials to optimize the blade structure. Also, it will optimize the wind blade to reach high stiffness with minimum weight. It will certainly minimize the cost of the wind turbine and improve its performance. Table 2 shows the properties of the three selected materials used to optimize the wind turbine blade [24,25].

Table 2. Material properties of wind turbine blade.

Material	E-Glass/Epoxy [24]	Carbon/Epoxy [24]	Braided Composite [24,25]
E_1 (GPa)	48.7	136.7	62.8
E_2 (GPa)	16.8	8.2	62.8
G_{12} (GPa)	5.83	4.45	9.68
G_{23} (GPa)	6	2.91	7.97
v_{12}	0.28	0.29	0.33
v_{23}	0.20	0.42	0.40
X_T (MPa)	1170	1604	460
X_C (MPa)	977	1305	420.4
Y_T (MPa)	30.5	40.5	526.2
Y_C (MPa)	114	239.7	420.4
ρ(kg/m^3)	2000	1518	1800

The blade of a small wind turbine consists of four basic parts: the root, the neck, the shell, and the shear web. Each part of the blade has a different layer thickness and fiber orientation. Determining proper fiber orientation and laminate thickness is significant in decreasing the difficulties of manufacturing and increasing the structural stiffness. The lay-up sequence, orientation, and laminate thickness are optimized for the selected composite materials. Table 3 presents the layers sequence of the blade, and Figure 5 shows the 3D model of wind turbine blade materials. Where each section is marked with diffident color. These colors reflect the difference in the thickness and fiber orientation of the composite material (Table 3).

Table 3. The lay-up sequence of 2.5 m small wind turbine.

Section Name	Location (m)	Shell Layup	Thickness (m)	Shear Web Lay-Up	Thickness (m)
1	0.200–0.400	[(±45)3/08/(±45)]s	0.0064	[(±45)3/09/(±45)]s	0.0070
2	0.400–0.600	[(±45)3/07/(±45)]s	0.0058	[(±45)3/08/(±45)]s	0.0064
3	0.600–0.811	[(±45)3/06/(±45)]s	0.0052	[(±45)3/07/(±45)]s	0.0058
4	0.811–1.022	[(±45)2/06/(±45)]s	0.0048	[(±45)3/06/(±45)]s	0.0052
5	1.022–1.233	[(±45)2/05/(±45)]s	0.0042	[(±45)2/06/(±45)]s	0.0048
6	1.233–1.444	[(±45)2/04/(±45)]s	0.0036	[(±45)2/05/(±45)]s	0.0042
7	1.444–1.655	[(±45)2/03/(±45)]s	0.0030	[(±45)2/04/(±45)]s	0.0036
8	1.655–1.866	[(±45)2/02/(±45)]s	0.0024	[(±45)2/03/(±45)]s	0.0030
9	1.866–2.077	[(±45)/02/(±45)]s	0.0020	[(±45)2/02/(±45)]s	0.0024
10	2.077–2.288	[(±45)/01/(±45)]s	0.0014	[(±45)/02/(±45)]s	0.0020
11	2.288–2.500	[(±45)/01/(±45)]	0.0007	[(±45)/01/(±45)]s	0.0014
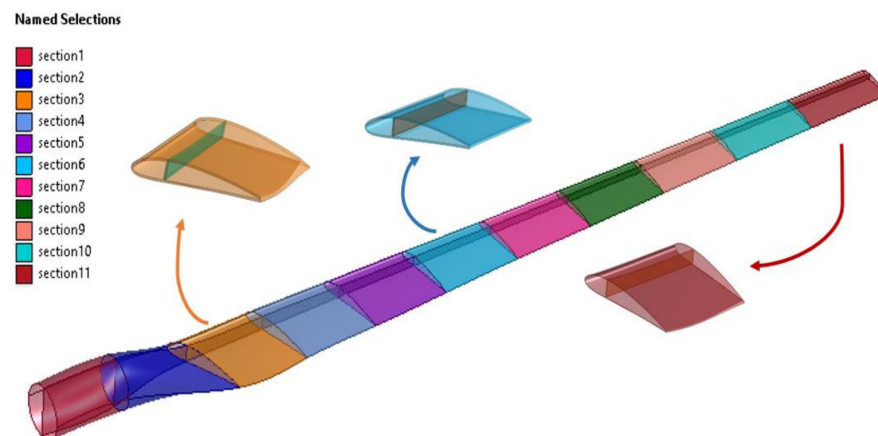
Figure 5. 3D model of the composite blade with 10 sections.

### 2.3. Finite Element Analysis of Steady-State Problem

The finite element model of the wind turbine blade was created using the Ansys software to study the steady-state structural problem. This simulation aims to select the most optimal material for the wind turbine blade under the aerodynamic loads. The output results of this analysis present the tip deflection, von-mises stress, and deformation. Computational fluid dynamics (CFD) was used (Ansys software) to calculate the aerodynamic loads, but this analysis requires a high-performance computer and consumes time [26]. Therefore, using the QBlade software based on BEM theory to calculate the aerodynamic loads can save time and effort. Table 4 presents the results of the applied loads on the wind turbine blade.

Table 4. The normal and tangential loads applied in the FE model.

$Z\ (m)$	$\Delta Z\ (m)$	$F_T(N/m)$	$F_N(N/m)$
0.200	0.200	−1.535	2.930
0.400	0.200	−4.415	8.825
0.600	0.200	27.610	57.455
0.811	0.211	38.052	81.014
1.022	0.211	36.047	93.246
1.233	0.211	35.260	106.279
1.444	0.211	34.701	120.023
1.655	0.211	34.492	134.815
1.866	0.211	33.881	147.971
2.077	0.211	32.781	161.331
2.288	0.211	29.654	172.156
2.500	0.212	9.8160	81.7452

2.4. Boundary Conditions

The blade of the wind turbine is fixed at the root side, so it was considered that all degrees of freedom (DOF) are null at the root, and on the tip, the blade is free to move. The blade rotates at a constant rotational speed during the analysis. The applied pressure is distributed over the shell of the blade. But the loads were calculated by the BEM theory applied at the center of the loads for each section of the blade. It was considered the force of gravity in the center of gravity of the blade mass. The loads and boundary conditions that are applied to the wind blade are shown in Figure 6.
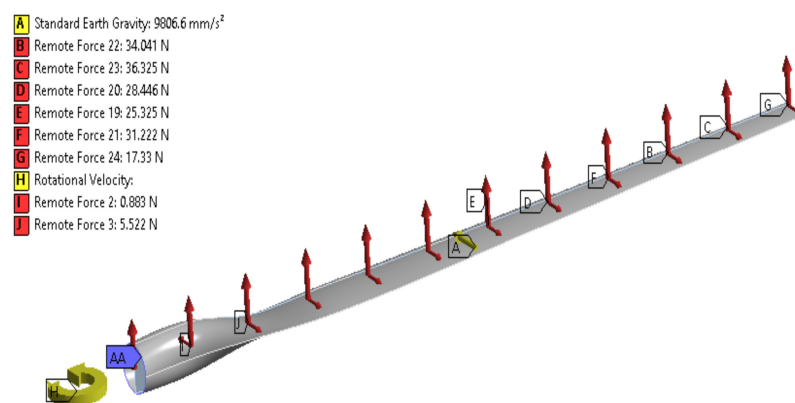

Figure 6. Boundary conditions and applied loads.

2.5. FE Modeling of Wind Blade

During the operation of the wind turbine blade, it is subjected to several loads, which leads to occur the bending and deflection of the blade. In order to simulate the wind turbine blade, the appropriate mesh should be chosen to match the geometry and material composition. In this study, it was selected the element (shell 281) to build the FE model. This element has eight nodes, and each node has six DOF. The Grid Independence Test was achieved to find the wind turbine blade's most optimal mesh, as shown in Table 5. Figure 7 shows the most optimal mesh of the wind blade.

Table 5. The mesh convergence of wind turbine blade.

Mesh Segments	No. Nodes	No. Elements	Max. Total Deflection [mm]	Difference
1	19,824	3694	18.392	-
2	26,722	7431	18.371	−0.021
3	34,624	11,385	18.365	−0.006
4	45,857	15,124	18.361	−0.004
5	74,154	24,475	18.356	−0.005
6	108,789	35,970	18.354	−0.002
7	225,602	75,053	18.358	0.004
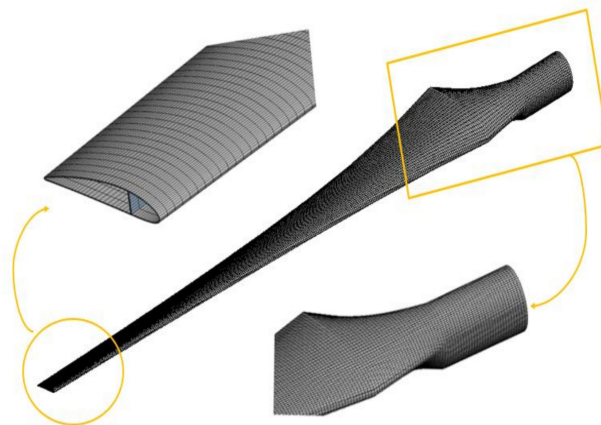
Figure 7. FE model wind turbine mesh.

2.6. The FE Formulation

The finite element can be applied to solve the modal analysis problem using the following equation to determine the steady-state response of wind turbine blades [27,28]:

$$[K]\{u\} = \{F\} \tag{7}$$

where $\{F\}$ is load vector, $\{u\}$ is displacement vectors, and $[K]$ is the stiffness matrix of the system. In Equation (7), it was assumed that the inertia forces and damping forces are equal to zero. Suppose a structure is placed in a suitable position at a zero moment in time, where the structure can be vibrated. This Vibration is known as the natural frequency, and this frequency follows certain patterns known as distortion patterns called mode shapes. The mode shapes and Vibration of the structure depend on mass and stiffness [27]. Assuming that the external force vector and the damping are zero, where the free vibration equation can be written as [28]:

$$[M]\{\ddot{u}\} + [K]\{u\} = 0 \tag{8}$$

where $[M]$ is the mass matrix, $\{\ddot{u}\}$ is the acceleration vector. Equation (8) is the equation of motion of the undamped free vibration system. In order to solve the last equation, the harmonic solution is assumed in the following form:

$$\{u\} = \{\varnothing\} \sin \omega t \tag{9}$$

where ω is the natural angular frequency of mode and $\{\varnothing\}$ is the vector of contractual amplitude for mode shapes. After deriving the displacement in Equation (9) twice with respect to time, it can be got the following:

$$\{\ddot{u}\} = -\omega^2 \{\varnothing\} \sin \omega t \tag{10}$$

Substitute Equations (9) and (10) into Equation (8) to get the following formula:

$$\left([K] - \omega^2[M]\right)\{\varnothing\} = 0 \tag{11}$$

Equation (11) is the form of the eigenvalue problem (structural Vibration). It is a set of homogeneous algebraic equations for the eigenvector components. The eigenvalue problem can be written as follows:

$$([A] - \lambda[I])\,X = 0 \tag{12}$$

where $[A]$ is a symmetric matrix or dynamic matrix, λ is the value of eigenvalue, $[I]$ is an identity matrix, and X is an eigenvector. By substituting Equation (11) into Equation (12) by entering one of the two matrices $[K]$ or $[M]$, and then using the Cholisky method (square root method), it can be obtained the dynamic response [27].

3. Results and Discussions

The main target of the optimization process of the wind turbine blade is to find the most optimal design to obtain the maximum power. The Betz method (BEMT) was used to design the primary chord and the twist angle of the blade, but one of the disadvantages of this method it's does not adopt the linear design of the chord and the twist angle. This analysis should be optimized the wind blade according to the linearization approach. Figure 8 shows the initial and the final optimum blade design.
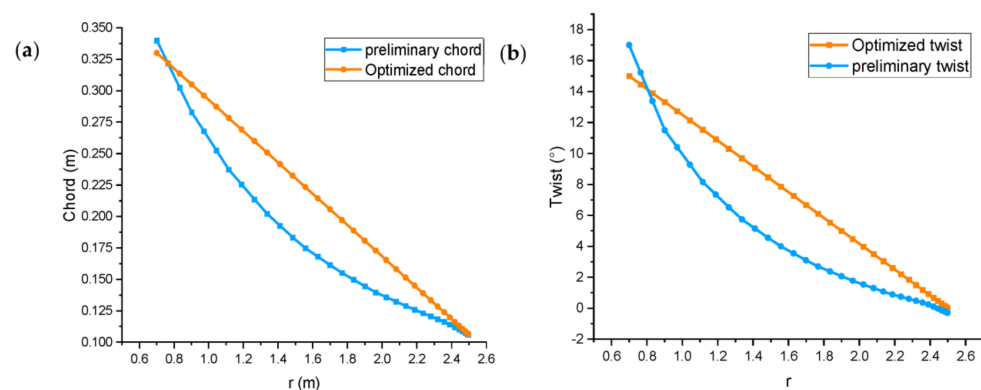

Figure 8. Blade distribution (**a**) chord Length and (**b**) twist angle.

Figure 8 shows the difference between the initial design based on the Betz theory (BEM), which is a parabolic curve, and the new design (improved). The improved design is based on the linearization design, where it is a straight line from the root to the tip for both the chord and the twist angle. Figure 9 shows the initial and optimized wind turbine design's power coefficient and power curve.
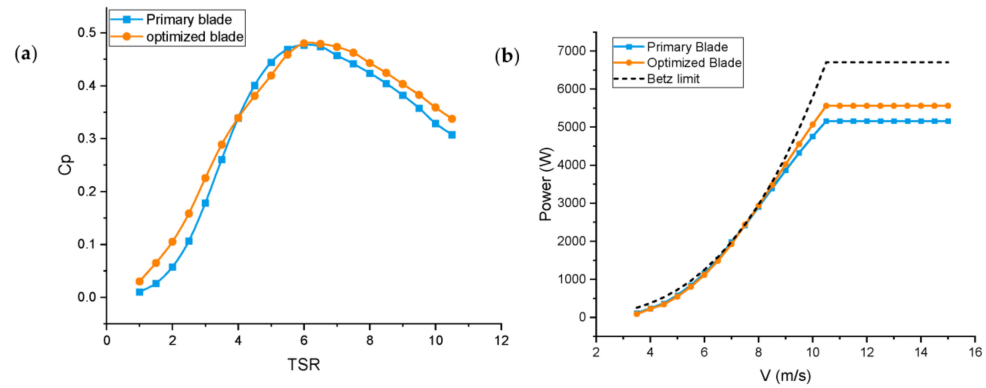
Figure 9. (**a**) power coefficient with tip speed ratio, (**b**) Power output with wind speed.

It can be noticed from Figure 9 that there is an increase in the power coefficient of the improved design. Where the power coefficient increased at the low TSR from 1 to 4 and is close to the initial design at the medium values of TSR. Later on, the power coefficient decreased for the TSR values greater than 6. This means that the improved design increased the power coefficient at low and high rotational speeds with an average increase of up to 8%. According to the obtained results in Figure 9, it can be concluded that the effect of improving the design to increase the power of the wind turbine is evident at the medium wind speed that starts from 8 m/s, and the improvement in the power at the rated wind speed is 7% compared with the initial design.

The steady-state finite element model was used to determine the variation of blade tip deflection and the Von Mises stresses of the wind blade using three different materials to find the most optimal material (with minimum tip deflection). Also, the zones of stress concentration of the blade structure can be determined, and the structure's strength can be improved to obtain an optimal wind blade. Figure 10 shows the distribution of Von-Mises stresses of the wind blade using the proposed materials. Figure 11 shows the distribution of deflection (tip deflection) of the wind turbine blade using different materials.
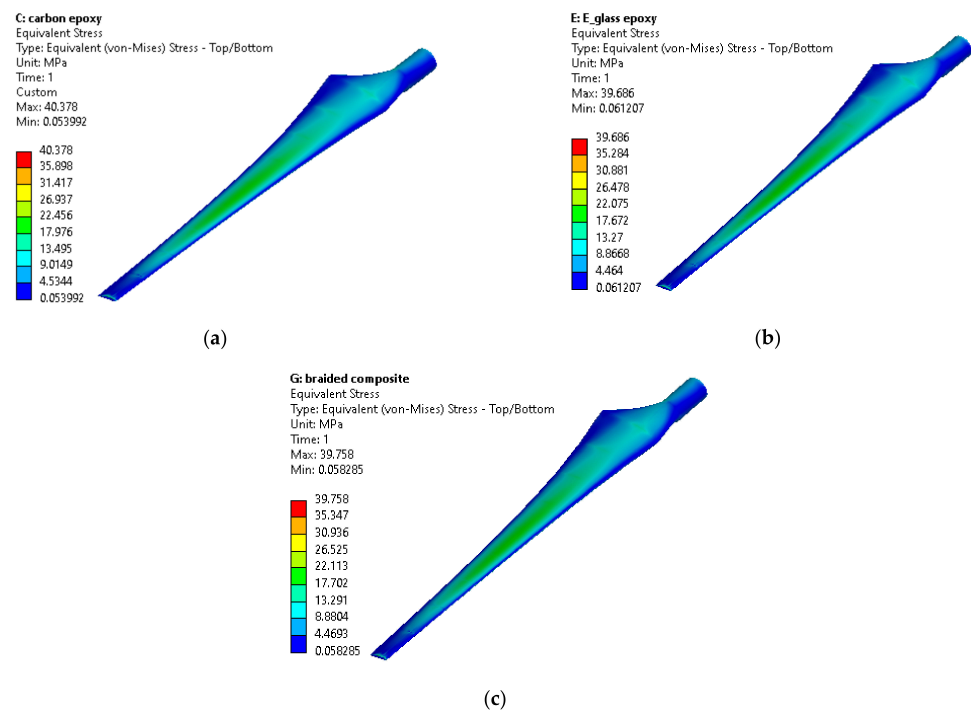

Figure 10. Distribution of Von Mises stresses of (**a**) carbon/epoxy, (**b**) E-glass/epoxy, and (**c**) Braided composite.
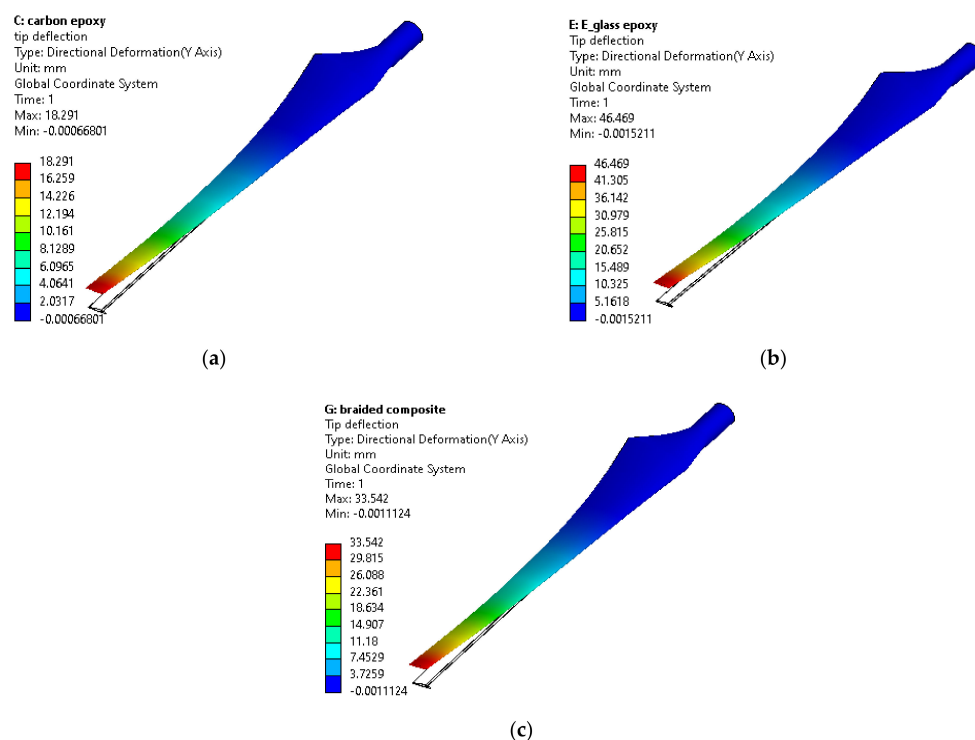
Figure 11. Tip deflections of (**a**) carbon/epoxy, (**b**) E-glass/epoxy, and (**c**) Braided composite.

In order to verify the selected approach to analyze the blade of a wind turbine, the comparisons between the results of QBlade software and ANSYS software were made to determine the tip deflection and Von-Mises stresses. High agreement was found between the results of QBlade software and ANSYS software, as shown in Table 6.

Table 6. The tip deflections and von mises stress using different materials.

	E-Glass/Epoxy			Braided Composite			Carbon/Epoxy		
	QBlade	ANSYS	Difference %	QBlade	ANSYS	Difference %	QBlade	ANSYS	Difference %
Von mises stress [MPa]	38.51	39.68	2.94	39.20	39.75	1.38	39.96	40.37	1.015
Tip deflection [mm]	43.20	46.46	7.016	29.32	33.54	6.61	16.86	18.29	7.81

According to the results of Figure 11, it can be seen that the blade bends in the direction of the lift forces due to the low pressure on this side. The Von-Mises stresses for glass fibers and carbon fibers are 39.68 MPa and 40.37 MPa, respectively. Where they are greater than the Von-Mises stresses for the braided composite material (39.75 MPa). It can be noticed that the maximum stresses are concentrated in the middle of the wind turbine blade length, and this indicates that the distribution of the fibers and the thickness is suitable for the structure. Regarding the tip deflection, Figure 11 shows a noticeable difference between the three blades that used different materials. The carbon fiber deflection was 18.29 mm, the glass fiber deflection was 46.46 mm, and the Braided composite deflection was 33.54 mm. However, these results for all cases remain acceptable, where the given distance between the tower and the tip of the blade is about 400 mm, which makes the three materials usable. But the low cost of E-glass compared to the other two materials makes it the most suitable material to manufacture the wind blade. Figure 12 shows the variations of blade deflections and Von-Mises stresses along the blade length, respectively. Figure 13 illustrates the distributions of mass along the blade length and the stiffness distribution using the three different materials under the same working condition.
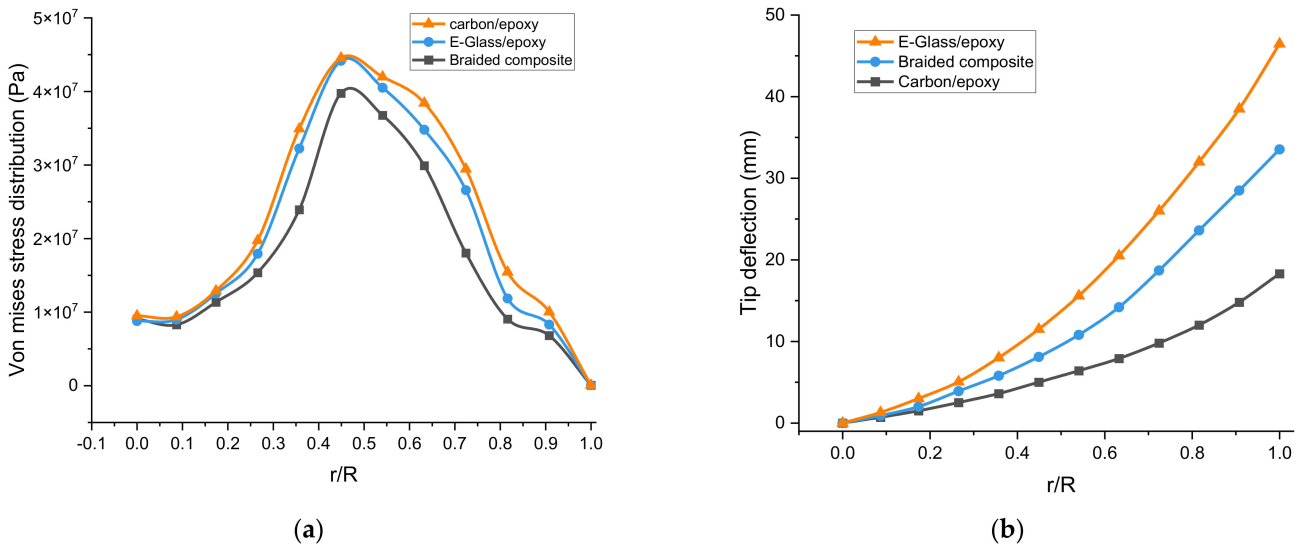
Figure 12. Variations of (**a**) Von mises stress and (**b**) tip deflection along the blade.
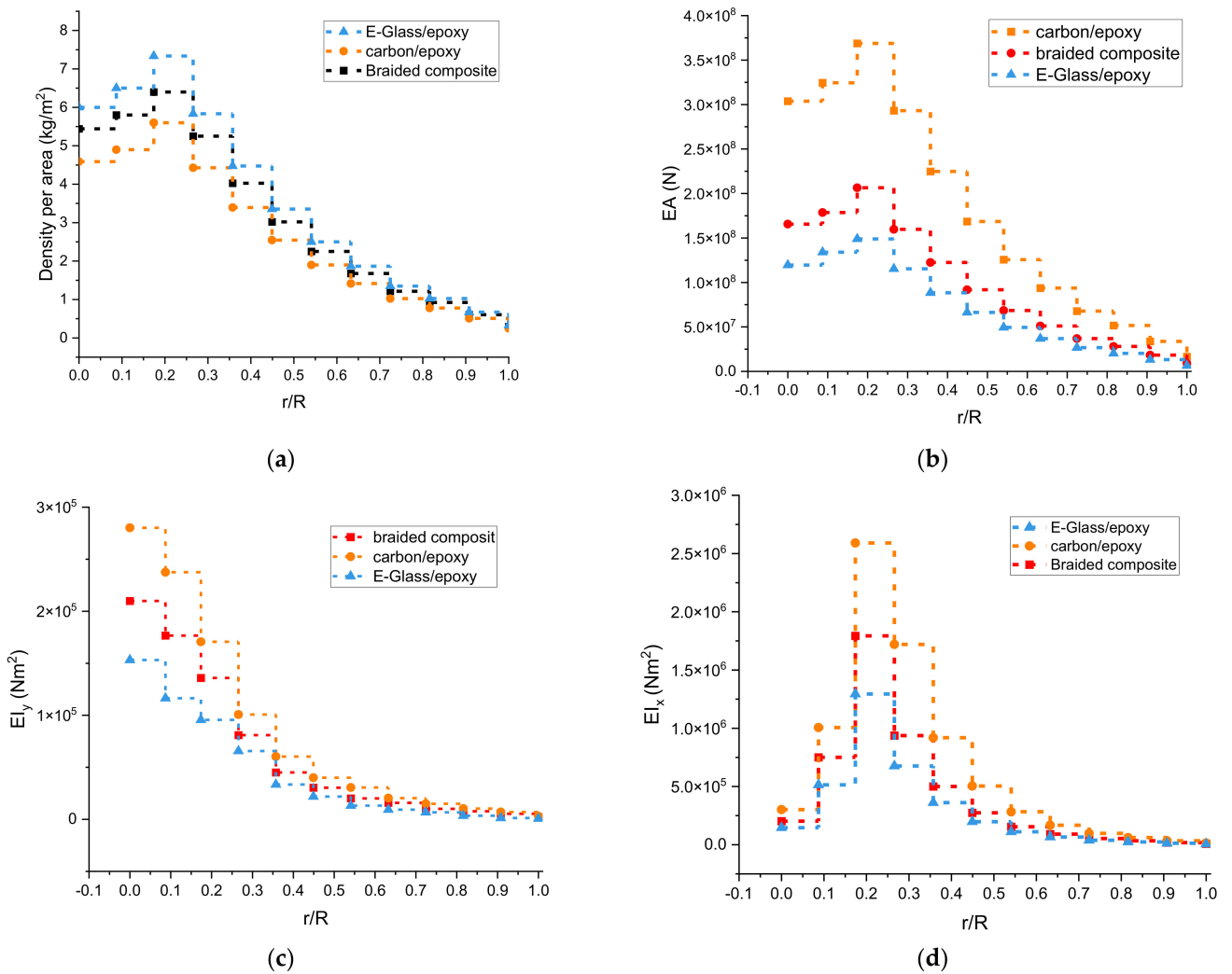

Figure 13. Distributions of (**a**) the density, (**b**) longitudinal stiffness, (**c**) Flapwise Stiffness, and (**d**) Edgewise Stiffness along the blade.

Based on the results of Figure 12, it can be seen that the largest value of the stresses occurred at $r/R = 0.5$, i.e., in the middle of the blade. This is accrued because the thickness distribution of the shell at the root is appropriate. This causes the stress concentration in the middle of the blade, i.e., in the area of least damage and risk. While results of Figure 12b showed that the largest deflection occurred for E-glass material, followed by braided composite material, and then carbon epoxy material. Figure 13 shows the wind turbine blade's distributions of mass and stiffness. It is clear that this distribution was linear, thicker on the root side and less thick on the tip side. This makes it a suitable distribution for the composite materials layers along the length of the blade.

The main objective of studying the dynamic problem of the wind blade is to determine the compatibility of the aerodynamic shape design with the structure of the blade or the status of mass distribution/stiffness that is appropriate along the length of the blade. The optimal mesh was selected depending on the mesh of the steady-state analysis, as shown in Figure 7. Figure 14 presents the natural frequencies and the displacements of the wind turbine blade for the first 6th mode shapes using the selected materials, respectively. Figures 15–17 show the first 6th mode shapes of the wind turbine blade using the selected materials. It A comparison was made between the results of Ansys software and QBlade to find the frequencies for different materials, as shown in Table 7.
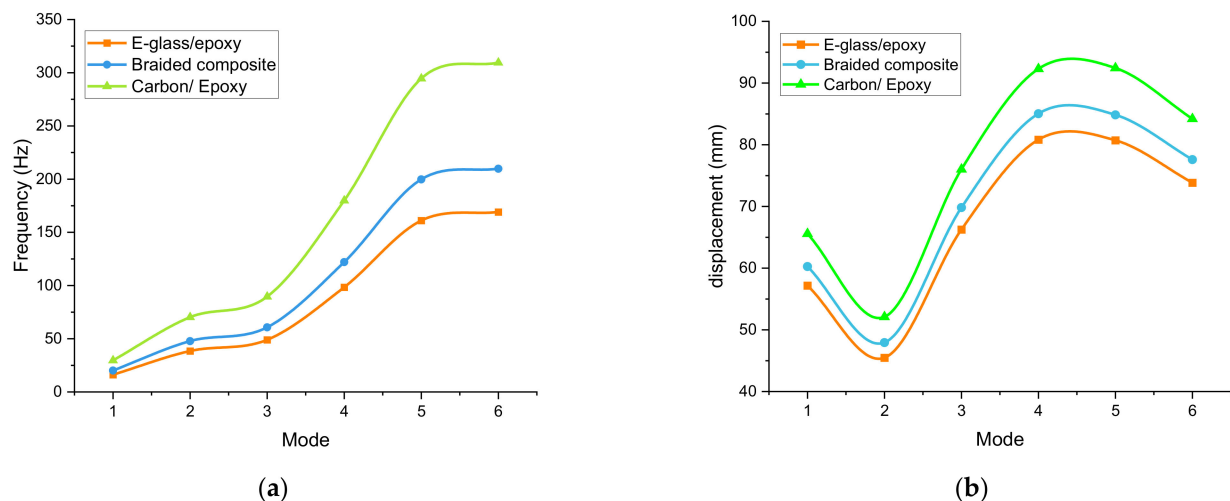

**Figure 14.** The variation of (**a**) natural frequency and (**b**) displacement with modes.

The wind turbine blade's structural stiffness depends on the materials' properties, especially Young's modulus (E) and the density (ρ). Therefore, the natural frequencies of the wind turbine structure depend basically on the ratio ($\sqrt{E/\rho}$). According to the results of the modal analysis of the wind turbine blade in Figure 14a, it's observed that the frequencies of the E-glass fiber material were less than those of braided composite and carbon epoxy materials, which made it less resistant to vibrations. Despite this, the braided composite and E-glass material results are not considered far away due to the convergence of their ratio ($\sqrt{E/\rho}$). While the carbon/epoxy material has the highest natural frequencies compared with the other materials because it has the highest ratio of ($\sqrt{E/\rho}$). Figure 14b shows the displacements of the blade tip at the selected modes shape of the three proposed materials. It can be seen that the carbon/epoxy material had the least displacement, due to the high stiffness of the material, followed by the braided composite material and then the E-glass/epoxy material. Also, it can be noticed that the highest value of the displacement occurred in the 4th and 5th modes, which makes them the two critical/dangerous modes for blade design.
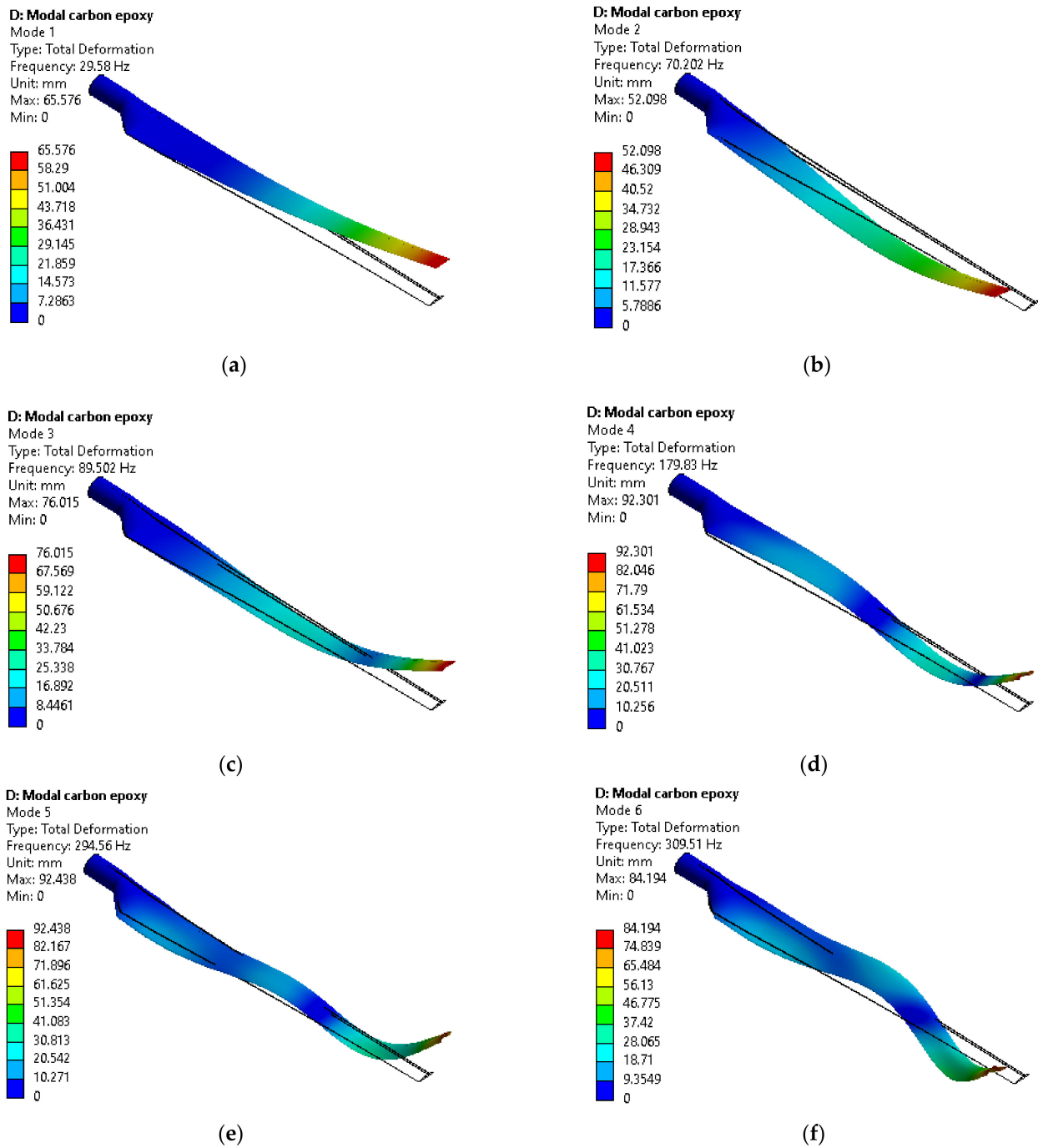
Figure 15. The first 6th mode shape of Carbon/Epoxy material. (**a**) 1st mode. (**b**) 2nd mode. (**c**) 3rd mode. (**d**) 4th mode. (**e**) 5th mode. (**f**) 6th mode.
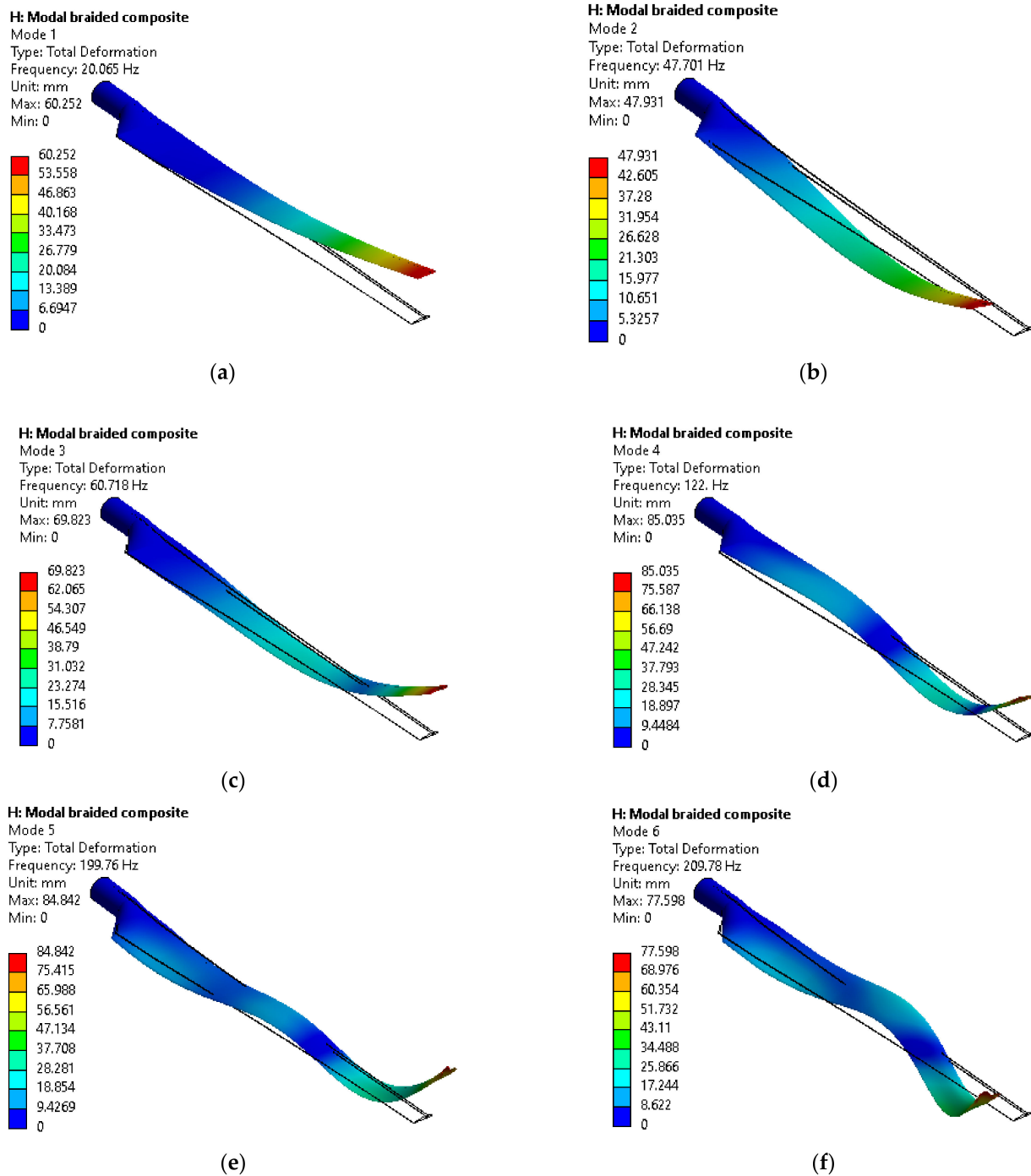
Figure 16. The first 6th mode shape of Braided composite material. (**a**) 1st mode. (**b**) 2nd mode. (**c**) 3rd mode. (**d**) 4th mode. (**e**) 5th mode. (**f**) 6th mode.
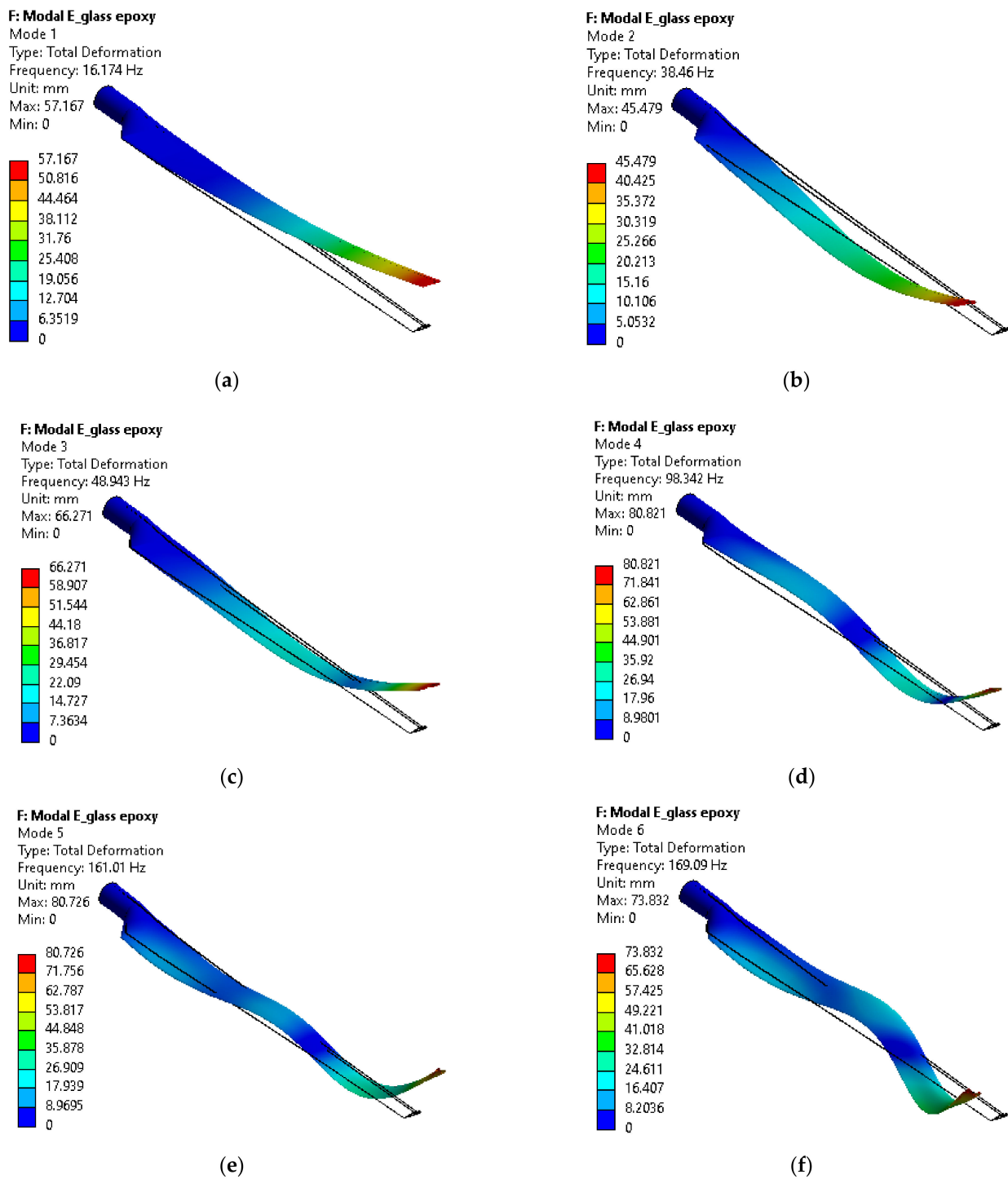
Figure 17. The first 6th mode shape of E-glass/epoxy material. (**a**) 1st mode. (**b**) 2nd mode. (**c**) 3rd mode. (**d**) 4th mode. (**e**) 5th mode. (**f**) 6th mode.

Table 7. The comparison of Frequencies using different materials.

Mode	E-glass/Epoxy			Braided Composite			Carbon/Epoxy		
	QBlade	ANSYS	Difference %	QBlade	ANSYS	Difference %	QBlade	ANSYS	Difference %
1	15.13	16.17	6.43	19.80	20.06	1.30	28.29	29.58	4.36
2	36.19	38.46	5.90	48.32	47.70	1.30	74.11	70.20	5.57
3	45.39	48.94	7.25	63.41	60.71	4.45	92.20	89.50	3.02
4	99.56	98.34	1.24	130.59	122	7.04	185.14	179.83	2.95
5	165.82	161.01	2.99	196.43	199.76	1.67	289.23	294.56	1.81
6	172.93	169.09	2.27	221.15	209.78	5.42	315.67	309.51	1.99

4. Conclusions and Future Work

In this study, a new model design of a small wind turbine (5 kW) was built from scratch. The main aim is to improve wind turbine aerodynamic characteristics and find the blade model's most optimal design parameters. It enhanced the power coefficient, reaching the value of 0.47 when TSR was equal to 6 for the optimal design. In other words, the efficiency increased by 8% compared to the initial design. At the same time, the power of the optimized wind turbine increased by 7% at rated wind speeds. A new finite element model was built for a small wind turbine blade of 5 kW based on the optimized wind turbine blade design. The steady-state and modal problems solutions were found to obtain the optimal material for the wind blade.

Further, it was found that the minimum tip deflections were 18.29 mm, 33.54 mm, and 46.46 mm, corresponding to the blade being made of carbon fiber material, Braided composite, and E-glass material, respectively. Hence, it can be concluded that the optimal material in terms of the magnitude of deflection is carbon fiber material. The modal analysis results showed that the natural frequencies of wind blade made from E-glass has the lowest natural frequencies (1st: 16.17 Hz and 2nd: 38.46 Hz). On the other hand, the wind blade made of carbon fiber has the largest natural frequencies (1st: 29.58 Hz and 2nd: 70.20 Hz).

In future works, some important problems should be investigated deeply. Fatigue is one of the main failure problems of wind turbine blades during operating periods, especially when it has a crack in the structure [29]. So, it's necessary to study the fatigue of the wind turbine using different materials under normal and extreme operating conditions. In recent research, nanotechnology has been adopted to improve composite materials [30]. This composite material can be applied to small wind turbines to enhance their efficiency. The other problem of wind turbines that should be investigated is the annoying sounds and noise during rotation in order to reduce it.

The climate of the locations of wind turbines varies from one site to another, from very hot to very cold. Thus, the study of the influence of climate on the dynamic characteristics of the wind turbine blade [31] is considered an essential issue as well.

Nomenclature

c	Chord length
C_P	Power coefficient
Re	Reynolds number
U_{rel}	Relative velocity
U_{design}	Design wind speed
r	Local radius
R	Wind turbine radius
$C_{l,design}$	Design lift coefficient
B	Number of blades
F_T	Tangential load
F_N	Normal load
$\{F\}$	Load vector
$\{u\}$	Displacement vectors
[K]	Stiffness matrix
[M]	Mass matrix
$\{\ddot{u}\}$	Acceleration
[A]	dynamic matrix
[I]	Identity matrix
X	eigenvector
E	Young's modulus

Greek symbols

θ	Twist angel
$\{\varnothing\}$	Reynolds or turbulent stress
μ	viscosity
ω	angular natural frequency
ρ	Air density
α_{opt}	Optimal angel of attack
λ_r	Local speed ratio
λ_0	Design tip speed ratio
φ	Relative angle
Ω	Rotational speed

Superscripts

WWEA	World wind energy association
GWEC	Global wind energy council
AEP	Annual energy production
FEM	Finite element method
UD	Unidirectional
BEM	blade element momentum
AoA	Angle of Attack
DOF	degrees of freedom
HAWT	Horizontal axis wind turbine
CFD	computational fluid dynamics

References

1. Rosato, M.A. *Small Wind Turbines for Electricity and Irrigation: Design and Construction*; CRC Press: New York, NY, USA, 2018.
2. WWEA. World Wind Energy Association. Available online: https://wwindea.org/information-2/statistics-news/ (accessed on 24 March 2022).
3. Rašuo, B.P.; Bengin, A.Č. Optimization of wind farm layout. *FME Trans.* **2010**, *38*, 107–114.
4. Norouzi, N.; Bozorgian, A. A Wind-Thermal System Design Based on an Energetic and Exergetic Approch. *Iran. J. Chem. Chem. Eng.* **2022**. [CrossRef]
5. Win, S.Y.; Thianwiboon, M. Parametric optimization of NACA 4412 airfoil in ground effect using full factorial design of experiment. *Eng. J.* **2021**, *25*, 9–19.
6. Mousavi, S.M.; Shafiei, N.; Dadvand, A. Numerical simulation of subsonic turbulent flow over NACA0012 airfoil: Evaluation of turbulence models. *Sigma J. Eng. Nat. Sci.* **2017**, *35*, 133–155.

7. Garcia-Ribeiro, D.; Flores-Mezarina, J.A.; Bravo-Mosquera, P.D.; Cerón-Muñoz, H.D. Parametric CFD analysis of the taper ratio effects of a winglet on the performance of a Horizontal Axis Wind Turbine. *Sustain. Energy Technol. Assess.* **2021**, *47*, 101489. [CrossRef]

8. Bai, C.-J.; Wang, W.-C. Review of computational and experimental approaches to analysis of aerodynamic performance in horizontal-axis wind turbines (HAWTs). *Renew. Sustain. Energy Rev.* **2016**, *63*, 506–519. [CrossRef]

9. Maizi, M.; Mohamed, M.; Dizene, R.; Mihoubi, M. Noise reduction of a horizontal wind turbine using different blade shapes. *Renew. Energy* **2018**, *117*, 242–256. [CrossRef]

10. Kaya, M.N.; Kose, F.; Ingham, D.; Ma, L.; Pourkashanian, M. Aerodynamic performance of a horizontal axis wind turbine with forward and backward swept blades. *J. Wind. Eng. Ind. Aerodyn.* **2018**, *176*, 166–173. [CrossRef]

11. Parezanovic, V.; Rasuo, B.; Adzic, M. Design of airfoils for wind turbine blades. In Proceedings of the French-Serbian European Summer University: Renewable Energy Sources and Environment-Multidisciplinary Aspect, Vrnjacka Banja, Serbia, 17–24 October 2006.

12. Song, F.; Ni, Y.; Tan, Z. Optimization design, modeling and dynamic analysis for composite wind turbine blade. *Procedia Eng.* **2011**, *16*, 369–375. [CrossRef]

13. Lipian, M.; Czapski, P.; Obidowski, D. Fluid–structure interaction numerical analysis of a small, urban wind turbine blade. *Energies* **2020**, *13*, 1832. [CrossRef]

14. Boudounit, H.; Tarfaoui, M.; Saifaoui, D.; Nachtane, M. Structural analysis of offshore wind turbine blades using finite element method. *Wind Eng.* **2020**, *44*, 168–180. [CrossRef]

15. Wu, W.H.; Young, W.B. Structural analysis and design of the composite wind turbine blade. *Appl. Compos. Mater.* **2012**, *19*, 247–257. [CrossRef]

16. Pourrajabian, A.; Afshar, P.A.N.; Ahmadizadeh, M.; Wood, D. Aero-structural design and optimization of a small wind turbine blade. *Renew. Energy* **2016**, *87*, 837–848. [CrossRef]

17. Tüfekci, M.; Genel, Ö.E.; Tatar, A.; Tüfekci, E. Dynamic Analysis of Composite Wind Turbine Blades as Beams: An Analytical and Numerical Study. *Vibration* **2021**, *4*, 1–15. [CrossRef]

18. Navadeh, N.; Goroshko, I.; Zhuk, Y.; Etminan Moghadam, F.; Soleiman Fallah, A. Finite Element Analysis of Wind Turbine Blade Vibrations. *Vibration* **2021**, *4*, 310–322. [CrossRef]

19. Lagdani, O.; Tarfaoui, M.; Nachtane, M.; Trihi, M.; Laaouidi, H. Modal analysis of an iced offshore composite wind turbine blade. *Wind Eng.* **2022**, *46*, 134–149. [CrossRef]

20. Puterbaugh, M.; Beyene, A. Parametric dependence of a morphing wind turbine blade on material elasticity. *Energy* **2011**, *36*, 466–474. [CrossRef]

21. Alkhabbaz, A.; Yang, H.-S.; Weerakoon, A.S.; Lee, Y.-H. A novel linearization approach of chord and twist angle distribution for 10 kW horizontal axis wind turbine. *Renew. Energy* **2021**, *178*, 1398–1420. [CrossRef]

22. Gupta, M.K.; Subbarao, P. Design and Performance Analysis of Hydrokinetic Turbine with Aerodynamic Stall Model. In *Advances in Thermofluids and Renewable Energy*; Springer: Singapore, 2021; pp. 221–231.

23. Marten, D.; Wendler, J. *QBlade Guidelines v0.6*; TU Berlin: Berlin, Germany, 2013.

24. Zhou, S.; Wu, X. Fatigue life prediction of composite laminates by fatigue master curves. *J. Mater. Res.* **2019**, *8*, 6094–6105. [CrossRef]

25. Gao, X.; Yuan, L.; Fu, Y.; Yao, X.; Yang, H. Prediction of mechanical properties on 3D braided composites with void defects. *Compos. Part B Eng.* **2020**, *197*, 108164. [CrossRef]

26. Pagano, A. Aerodynamic Analyses of Tiltrotor Morphing Blades. In *Morphing Wing Technologies*; Elsevier: Amsterdam, The Netherlands, 2018; pp. 799–839. [CrossRef]

27. Zuheir, S.; Abdullah, O.I.; Al-Maliki, M. Stress and vibration analyses of the wind turbine blade (A NREL 5MW). *J. Mech. Eng. Res. Dev.* **2019**, *42*, 14–19. [CrossRef]

28. Garinis, D.; Dinulović, M.; Rašuo, B. Dynamic analysis of modified composite helicopter blade. *FME Trans.* **2012**, *40*, 63–68.

29. Abdullah, O.I. A finite element analysis for the damaged rotating composite blade. *Al-Khwarizmi Eng. J.* **2011**, *7*, 56–75.

30. Miau, J.-J.; Li, S.-R.; Tsai, Z.-X.; Van Phung, M.; Lin, S.-Y. On the aerodynamic flow around a cyclist model at the hoods position. *J. Vis.* **2019**, *23*, 35–47. [CrossRef]

31. Abdullah, O. Vibration analysis of rotating pre-twisted cantilever plate by using the finite element method. *J. Eng.* **2009**, *15*, 3492–3505.